

A Local Galilean Invariant Thermostat

Robert D. Groot*

Unilever Research Vlaardingen, P.O. Box 114, 3130 AC Vlaardingen, The Netherlands

Received November 3, 2005

Abstract: The thermostat introduced recently by Stoyanov and Groot (*J. Chem. Phys.* **2005**, *122*, 114112) is analyzed for inhomogeneous systems. This thermostat has one global feature, because the mean temperature used to drive the system toward equilibrium is a global average. The consequence is that the thermostat locally conserves energy rather than temperature. Thus, local temperature variations can be long-lived, although they do average out by thermal diffusion. To obtain a faster local temperature equilibration, a truly local thermostat must be introduced. To conserve momentum and, hence, to simulate hydrodynamic interactions, the thermostat must be Galilean invariant. Such a local Galilean invariant thermostat is studied here. It is shown that, by defining a local temperature on each particle, the ensemble is locally isothermal. The local temperature is obtained from a local square velocity average around each particle. Simulations on the ideal gas show that this local Nosé–Hoover algorithm has a similar artifact as dissipative particle dynamics: the ideal gas pair correlation function is slightly distorted. This is attributed to the fact that the thermostat compensates fluctuations that are natural within a small cluster of particles. When the cutoff range r_c for the square velocity average is increased, systematic errors decrease proportionally to $r_c^{-3/2}$; hence, the systematic error can be made arbitrary small.

1. Introduction

To simulate complex liquids on microsecond time scales and length scales intermediate between the atomistic scale and the macroscopic scale, several techniques are available. In some techniques, an underlying lattice is used like in time-dependent Ginzburg–Landau theory^{1,2} and in Lattice Boltzmann simulations.^{3,4} Other techniques are particle-based, like Dissipative Particle Dynamics (DPD),^{5–7} Voronoi Dissipative Particle Dynamics,⁸ and Stochastic Rotation Dynamics.⁹ In a particle-based simulation, the time evolution of a set of interacting particles is followed by integrating their equations of motion according to the laws of classical mechanics. When particles interact by a pairwise potential only, the natural thermodynamic ensemble is the microcanonical *NVE* ensemble, where energy E is conserved. However, in many cases, it is desirable that the simulation generates an *NVT* ensemble, where T is the absolute thermodynamic temperature. To this end, a “thermostat” is applied to the system.

The Nosé–Hoover thermostat^{10,11} is a common choice for canonical molecular dynamic (MD) simulations. The basic idea behind this is to introduce a new internal degree of freedom into the Hamiltonian of the system H , representing the thermostat coupling. This in turn modifies the equations of motion and introduces one extra equation for the thermostat variable α , which has to be integrated together with the other equations:

$$m_i \frac{d\mathbf{r}_i}{dt} = \mathbf{p}_i; \quad \frac{d\mathbf{p}_i}{dt} = -\nabla_i U - \alpha \mathbf{p}_i; \quad \frac{d\alpha}{dt} = (T - T_0)/t_s \quad (1)$$

where \mathbf{p}_i is the momentum of particle i with mass m_i at position \mathbf{r}_i , T is the momentary value of the system temperature as defined above, $U(\mathbf{r}_i)$ is the potential energy of the system, and t_s is the thermostat coupling parameter (the rise time), which controls energy transfer back and forth from the thermostat. In the last equation, α acts as an effective friction parameter. MD simulations, in this case, are actually performed in a microcanonical *NVE'* ensemble, with modified Hamiltonian H' . Nevertheless, the thermody-

* Author e-mail: rob.groot@unilever.com.

dynamic averages in this NVE' ensemble are equivalent to an average in the canonical NVT ensemble for the original Hamiltonian H , but with rescaled particle momentum. This thermostat is global because the momentary value of the temperature is based on a global definition. Obviously, the Nosé–Hoover thermostat is non-Galilean invariant, because all calculations are performed in a reference frame in which the center of mass of the system is at rest. This is the only frame where velocity rescaling and particle friction relative to the coordinate frame preserve total momentum. This restriction also means that the thermostat is not suitable when external forces (like external pressure or gravity) are acting on the system and accelerating the center of mass. The thermostat effectively brings an additional external friction force, which means that hydrodynamics is artificial. The same holds for total angular momentum; if it is nonzero, the thermostat introduces an external friction torque. Generally, this thermostat does not conserve local (angular) momentum. These drawbacks are due to the fact that effective thermostating forces are noncentral and nonpairwise additive. These disadvantages are removed in the pairwise noise and friction thermostat that is implemented in DPD.^{5–8}

In the DPD method, pairwise additive and central forces are introduced: a dissipative force \mathbf{F}_{ij}^D and a random force \mathbf{F}_{ij}^R , which act together with the conservative force $-\nabla_i U$. These forces are tuned in such a manner so that the system evolution in phase space is governed by the Liouville equation, so that it obeys the fluctuation–dissipation theorem.⁶ By construction, the DPD thermostat is local and Galilean invariant and, therefore, preserves hydrodynamics. The main disadvantage of DPD is that the resulting stochastic equations of motion are difficult to integrate self-consistently.¹² Self-consistent integration requires several force calculations per time step, which decreases computational efficiency. An implementation that is not self-consistent⁷ (single force calculation per time step) leads to some artifacts. One of these is that the pair correlation function of the ideal gas deviates from 1,¹² which means that nonphysical interactions are present between particles. The second disadvantage of DPD is that it simulates fluids with comparable diffusion coefficient D and kinematic viscosity $\nu = \eta/\rho$, resulting in Schmidt numbers $Sc = \nu/D$ close to 1.⁷ Depending on the application, this could be a disadvantage, because for most common liquids the Schmidt number is on the order of 10^3 , but for diffusion-limited problems, this can be viewed as an advantage.

A completely different thermostat is the Andersen thermostat,¹³ which implements a Monte Carlo scheme to sample the equilibrium velocity distribution. The velocity of a randomly chosen particle is replaced by a velocity drawn from a Maxwell distribution. This thermostat is local by nature, but it does not preserve hydrodynamics. Recently, Lowe¹⁴ proposed a generalization of this as an alternative to DPD. The idea is to change the relative velocities of pairs of particles, rather than acting on single particles. To this end, the relative velocity is projected on the line connecting their centers, and this value is replaced by a value drawn from a Maxwell distribution. One might interpret this process as the exchange of a virtual particle between the two real

particles. It is the momentum carried by these virtual particles that causes a viscosity increase. By construction, the Lowe–Andersen thermostat is Galilean invariant, local, and preserves hydrodynamics. The viscosity of the fluid sampled with this thermostat is linearly proportional to the exchange frequency, which in turn determines thermostating efficiency. To have good thermostating, a relatively high exchange frequency must be used, which in turn leads to very viscous fluids. In some cases, this can be a disadvantage, because a low Schmidt number cannot be accessed.

Recently, a thermostat that is able to simulate both at low and at high Schmidt numbers was proposed by Stoyanov and Groot.¹⁵ This new thermostat also acts on pairs of particles, but at each time step, a random choice is made between the Lowe–Andersen thermostat and a local version of the Nosé–Hoover thermostat. Just as in DPD, a velocity-dependent pairwise force is introduced

$$\mathbf{F}_{ij} = \alpha \psi(r_{ij}/r_c) (1 - T/T_0) [(\mathbf{v}_i - \mathbf{v}_j) \cdot \mathbf{e}_{ij}] \mathbf{e}_{ij} / \delta t \quad (2)$$

where $\psi(r)$ is smooth smearing function and α is a fixed coupling parameter. The idea behind this is that particles will experience a friction force if the temperature is too high, but they are accelerated when the temperature is too low. Generally, when the system is close to equilibrium, the force in eq 2 (nearly) vanishes, so that this thermostat avoids the problems encountered in DPD to integrate the equations of motion. There is, however, a subtle point in this formulation which leads to a nonlocal interaction. This is that the temperature T is defined as a *global* average over local squared velocity differences. The consequence of this is that the thermostat switches off when the global temperature equals the temperature T_0 that is aimed for, even if the local temperature is too high in one part of the system and too low in another part. We will show below that this situation may arise in an inhomogeneous system, where the initial state is not in pressure equilibrium. Because of adiabatic expansion, one part of the system then cools while the other part heats. Such an off-equilibrium temperature distribution may pertain for a relatively long time until heat diffusion has equilibrated the system spontaneously. To force the system to the desired temperature throughout the system in such situations, a truly local thermostat is needed, based on a local definition of temperature. This will be described below.

2. Pairwise Nosé–Hoover Thermostat

The basic idea behind the Stoyanov–Groot thermostat is to combine two thermostats coupled in parallel. The first is a thermostat *similar* to the Nosé–Hoover thermostat (NHT)^{10,11} but which is Galilean invariant and acts on pairs of particles, rather than on single particles. The second is the Lowe–Andersen thermostat (LAT),¹⁴ which is a pairwise analogue of the Andersen thermostat.¹³ For each particle pair, a choice is made between NHT and LAT with probability $P = \Gamma \delta t$, where δt is the integration time step and Γ is the Lowe–Andersen exchange frequency. We will concentrate on the pairwise Nosé–Hoover thermostat here.

The pairwise analogue of the Nosé–Hoover thermostat is implemented by applying a thermostating force acting on

pairs of particles i and j within a cutoff distance r_c , as in eq 2. The coupling parameter α is constant during the simulation, unlike in the Nosé–Hoover thermostat. The advantage of this thermostat is that it conserves both total linear and angular momentum in the system, which is a necessary condition for restoring proper hydrodynamic behavior. A similar type of thermostating force was independently suggested recently by Phares and Srinivasa,¹⁶ for implementing molecular internal degrees of freedom in energy-conserving molecular dynamic simulations. In that implementation, the local internal temperature of particles i and j follows from a differential equation describing heat flow. In the formulation by Stoyanov and Groot,¹⁵ temperature is a local average of square velocity differences. To guarantee Galilean invariance, the temperature must be defined in a comoving frame for each particle. Within this frame, the local mean square velocity of the neighbors within a cutoff radius is determined. When the average is taken over all such determined local mean square velocities, the system temperature is defined as

$$kT = \frac{\sum_{i>j} \zeta(r_{ij}/r_c) M_{ij}(\mathbf{v}_i - \mathbf{v}_j)^2}{3 \sum_{i>j} \zeta(r_{ij}/r_c)} \quad (3)$$

where $\zeta(r)$ is a smearing function for the temperature, chosen such that $\zeta = 0$ for $r > 1$. The cutoff value r_c in the force (eq 2) and in the temperature (eq 3) could be different in principle. The parameter M_{ij} appearing in eq 3 is the reduced mass $m_i m_j / (m_i + m_j)$ of particles i and j . For particles of equal mass, $M_{ij} = 1/2$. Because at equilibrium the velocities and particle positions are independent, it is straightforward to prove that the above temperature definition coincides with the equilibrium thermodynamic temperature.

The fact that the momentary value of the temperature (eq 3) is calculated on the basis of all particle velocities and coordinates of the system leads to a global thermostat. As we will see later on, this subtle global nature of this thermostat is important for systems far from equilibrium. Therefore, we also define a truly local momentary temperature as

$$kT_i = \frac{\sum_j \zeta(r_{ij}/r_c) M_{ij}(\mathbf{v}_i - \mathbf{v}_j)^2}{3 \sum_j \zeta(r_{ij}/r_c)} \quad (4)$$

The thermostating force then can be modified so that it contains only local particle temperatures; hence

$$\mathbf{F}_{ij} = \alpha \psi(r_{ij}/r_c) [1 - 1/2(T_i + T_j)/T_0][(\mathbf{v}_i - \mathbf{v}_j) \cdot \mathbf{e}_{ij}] \mathbf{e}_{ij} / \delta t \quad (5)$$

However, in practice, MD simulations are usually performed with a relatively low particle density. This means that the local temperature defined through eq 4 is not very efficient in terms of temperature control, because of a large variance in the local temperature around its mean value. For such a local pairwise thermostat, the fluctuations around T_0 are typically an order of magnitude larger than that for the

thermostat based on a global temperature, if in both cases the same smearing function is chosen.¹⁵

3. The Global Temperature Problem

Why a global temperature definition does lead to problems when the thermostatic force of eq 2 is used can be illustrated by the following example. Let us take a simulation box of dimensions $30 \times 10 \times 10 r_c^3$, where r_c is the cutoff radius of the interaction that we shall take as our unit of length. The left half of this box is filled with 4500 A particles (leading to a mean density $\rho = 3$), and the right half of the box is filled with 1500 B₃ trimers. Each trimer is made by linking three B particles by harmonic springs with spring constant $C = 4$. The A and B particles interact with the soft potential

$$U_{ij} = \begin{cases} 1/2 a_{ij} (1 - r_{ij}/r_c)^2 & \text{if } r_{ij} < r_c \\ 0 & \text{if } r_{ij} > r_c \end{cases} \quad (6)$$

We take the repulsions $a_{AA} = a_{BB} = 25$ and $a_{AB} = 42$. Following Groot and Warren,⁷ this corresponds to a phase-separating system with χ parameter $\chi \approx 5$. This is such a low miscibility that no trimers dissolve in the A phase and only a fraction $\phi = 0.2\%$ of the A beads dissolve into the B phase. This implies that the two phases do not exchange particles in practice; they only exchange heat and momentum.

Because the trimer liquid lacks entropic degrees of freedom as compared to the monomer liquid of the same density, the pressure of a trimer liquid is lower by $2/3 \rho kT$, where ρ is the monomer density. Consequently, the equilibrium density of the B phase is higher than that of the A phase. The system is integrated using the standard velocity Verlet algorithm, using step size $\delta t = 0.05$, which is a safe step size for this potential. The pairwise Nosé–Hoover thermostat is used, based on a global temperature definition. When we start the simulation with equal densities of beads in both halves of the system, it starts off-equilibrium. In an adiabatic simulation (the natural ensemble when the thermostat is switched off), the A phase should cool under expansion, whereas the B phase should heat up. This is indeed observed to happen in the simulation. When the overall mean temperature, that is, the global temperature defined in eq 3, matches the desired temperature T_0 , the thermostat force in eq 2 effectively vanishes for all particle pairs. Consequently, the thermostat does not remove any local deviations from the desired temperature, and such temperature variations can thus persist for a long time. This is illustrated in Figure 1, where the temperature is plotted as function of the x coordinate through the simulation box, for three different evolution times: $t = 14\tau_0$, $39\tau_0$, and $114\tau_0$. The temperature profiles are averaged over 450 time steps around the mean evolution times. Note that we use the units of length, mass, and energy as $r_c = m = k_B T_0 = 1$, and thus, we have the unit of time $\tau_0 = r_c(m/k_B T_0)^{1/2} = 1$.

The interpretation of this result is that the trimer phase on the right-hand side of the system is heated adiabatically early on in the simulation, and that heat is slowly spreading afterward. Thus, the temperature variation should follow Laplace's law, $\partial\theta/\partial t = D_h \nabla^2 \theta$, where D_h is the heat diffusion

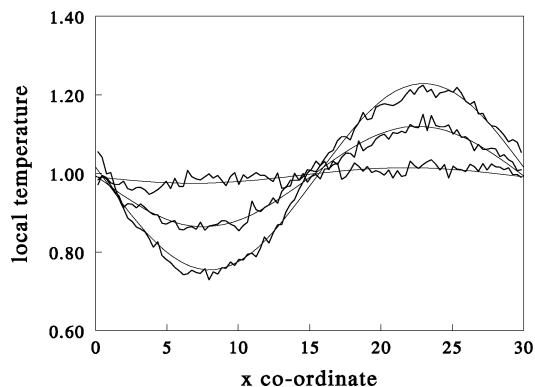


Figure 1. Temperature profile through the system at time $t = 14, 39$, and 114 .

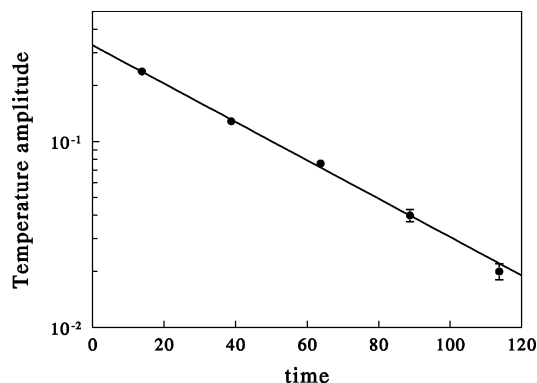


Figure 2. Amplitude of the temperature variation as a function of time. Error bars for the first points are within the size of the symbols.

constant and $\theta(x,t) = T(x,t) - T_0$. For a pure wave mode, this is solved by $\theta(x,t) = \theta_0 \exp(-t/\tau) \sin(kx)$, where $\tau^{-1} = D_h k^2$. To check this behavior, the local temperature variation is fitted to a sine function, and the amplitude is plotted as function of time in Figure 2. This shows that the amplitude indeed decays as a single exponential. From the decay time $\tau = 42 \pm 1$, we find a heat diffusion coefficient $D_h = L^2/4\pi^2\tau = 0.54 \pm 0.01$, where $L = 30$ is the system size in the x direction. This diffusion constant is comparable in size to the particle diffusion constant $D = 0.36 \pm 0.01$ and the kinematic viscosity $\nu = 0.26 \pm 0.01$ for single-particle systems with repulsion parameter $a = 25$. Although this behavior is physically quite reasonable, the problem now is that thermal equilibration in the system is essentially governed by heat transfer as far as temperature inhomogeneities are concerned. Thus, the response time depends on the system size as $\tau = L^2/4\pi^2 D_h \approx L^2/21$ for the present repulsion parameters. Hence, if a truly locally isothermal simulation is desired, the thermostat has to be adapted. This is described in the next section.

4. Local Nosé–Hoover Thermostat

As mentioned in section 2, a truly local pairwise Nosé–Hoover thermostat can be constructed on the basis of eqs 4 and 5, but this suffers from the large fluctuations in the local temperature T_i . To solve this problem, we need to define a slowly varying variable θ_i , which is a smoothed average over the local temperature T_i . Two options are open to obtain

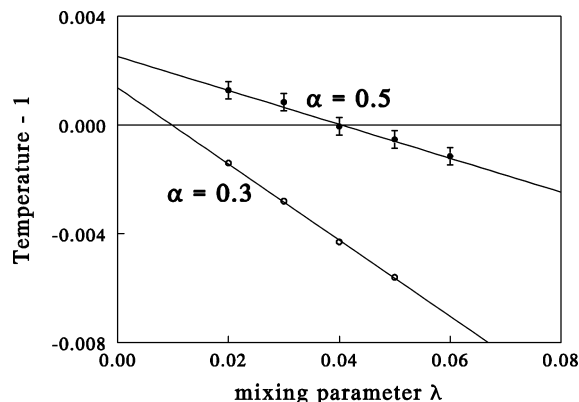


Figure 3. Temperature deviation from 1 for two values of the thermostat force, as a function of the mixing parameter.

such a slowly varying local temperature: by making a time average for each individual particle and by making a spatial average around each particle. The first option makes the thermostat slower. However, because the pairwise Nosé–Hoover thermostat based on a global temperature is an order of magnitude faster than DPD—it restores the correct temperature within a few MD steps—there is room to trade off thermostating speed for accuracy.

A time-averaged particle temperature can be defined following the update scheme:

$$\theta_i(t + \delta t) = (1 - \lambda) \theta_i(t) + \lambda T_i(t) \quad (7)$$

which is then substituted in the thermostat force

$$\mathbf{F}_{ij} = \alpha \psi(r_{ij}/r_c) [1 - \frac{1}{2}(\theta_i + \theta_j)/T_0][(\mathbf{v}_i - \mathbf{v}_j) \cdot \mathbf{e}_{ij}] \mathbf{e}_{ij} / \delta t \quad (8)$$

To test this thermostat, we used the weight functions $\psi(r) = \zeta(r) = (1 - r)$ for $r < 1$ and $\psi(r) = \zeta(r) = 0$ for $r > 1$; 3000 particles were simulated in a box of dimensions $10 \times 10 \times 10 r_c^3$ for the potential given in eq 6, with $a = 25$ and time step $\delta t = 0.05$. Parameter λ in eq 7 is a mixing parameter that determines the rise time of the thermostat $t_s \sim 1/\lambda$. This is analogous to the ordinary Nosé–Hoover thermostat, eq 1. In the actual implementation, the velocity correction for each particle is stored in an array $d\mathbf{v}_i$. The sum over neighbors is done in the force loop, where for each pair of neighboring particles $\mathbf{F}_{ij}\delta t$ (from eq 8) is added to $d\mathbf{v}_i$ and subtracted from $d\mathbf{v}_j$. In the final velocity update step, $d\mathbf{v}_i$ is added to the velocity of each particle.

For $\alpha = 0.3$ and 0.5 , the deviation of the temperature from its set value is shown in Figure 3. This shows that the deviations from the desired temperature are in the third digit. Moreover, the temperature decreases with λ , for both values of the thermostat force. This means that the thermostat is overdamped for too-small rise times and underdamped for too-large rise times. For a well-chosen value of the mixing parameter, the system is critically damped, which occurs at $\lambda \approx 0.01$ for $\alpha = 0.3$, $\lambda \approx 0.025$ for $\alpha = 0.4$, and $\lambda \approx 0.04$ for $\alpha = 0.5$.

Obviously, we would like to have critical damping so that the temperature is exactly the desired value, and we would like to have a fast response of the thermostat. But these two requirements are incompatible within this scheme. Moreover,

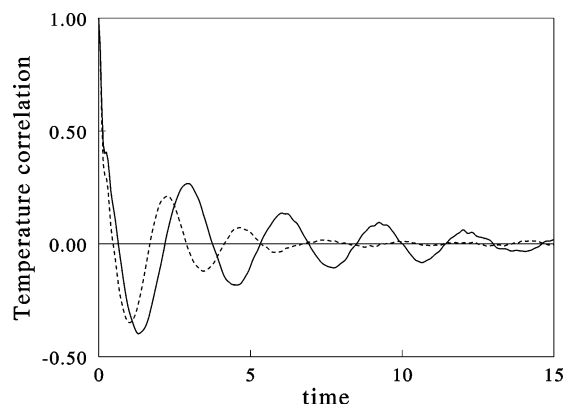


Figure 4. Temperature autocorrelation for $\alpha = 0.4$, averaged over 10^5 time steps, for $\lambda = 0.025$ and $\mu = 0.0$ (full curve) and for $\lambda = 0.05$ and $\mu = -0.01$ (dashed curve).

we find that the temperature autocorrelation function shows slowly decaying oscillations. An example is shown in Figure 4, for the parameters $\alpha = 0.4$ and $\lambda = 0.025$. To check if this problem is caused by oversteering, the force amplitude of the thermostat was lowered to $\alpha = 0.3$, and to maintain the same temperature, the mixing parameter was reduced to $\lambda = 0.01$. For these parameters, however, the oscillations in the correlation function do not disappear. To summarize, a straightforward generalization of the Nosé–Hoover thermostat to a purely local implementation does not lead to satisfactory results. The thermostat is typically slow and oscillatory.

To improve the performance of the thermostat, two scenarios have been studied. First, the local smoothed temperature on each particle is averaged over that of the neighboring particles to obtain a wider spatial average

$$\theta_i(t + \delta t) = (1 - \lambda - \mu) \theta_i(t) + \lambda T_i(t) + \mu \sum_j \xi(r_{ij}) \theta_j(t - \delta t) / \sum_j \xi(r_{ij}) \quad (9)$$

The last term is an average over the local smoothed temperature of the neighbors of particle i . Mixing the local mean temperature with the average neighbor temperature has the advantage that a spatial average is generated iteratively. However, the influence of parameter μ on the mean temperature and on the temperature autocorrelation function is quite small. In practical terms, this scheme does not lead to an improvement over eq 7 for the range $0 < \mu < 1$, and the correlation time remains large. Therefore, a variation of eq 9 has been studied, where the neighbor temperature is the measured temperature of the previous time step, rather than the smoothed temperature variable:

$$\theta_i(t + \delta t) = (1 - \lambda - \mu) \theta_i(t) + \lambda T_i(t) + \mu \sum_j \xi(r_{ij}) T_j(t - \delta t) / \sum_j \xi(r_{ij}) \quad (10)$$

This scheme works very well for $\alpha = 0.4$, $\lambda = 0.05$, and $\mu = -0.01$, that is, for a *negative* value of μ . The temperature thus obtained is $T = 0.999$, and the correlation time is $\tau = 2.1\tau_0$. This is 2.6 times faster than for $\mu = 0$, which is shown in Figure 4. For the same parameters, eq 9 leads to the same temperature, but to a longer correlation time, $\tau = 3.7\tau_0$. A

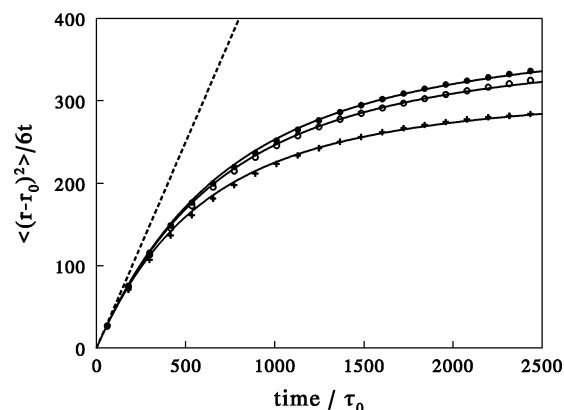


Figure 5. Mean square displacement for the ideal gas at density $\rho = 1$ (+), $\rho = 3$ (○), and $\rho = 10$ (●). The dashed curve is the ballistic result $\Delta^2/6t = 1/2 t$ for a divergent diffusion constant.

negative value for μ implies that the change in the smoothed temperature variable θ_i depends not only on the deviation of the local temperature from the smoothed temperature but also on its time derivative. This can, in turn, be interpreted as the mechanical work acting on a particle, as $dT_i/dt \approx 2/3 \langle M_{ij} \mathbf{v}_{ij} \cdot d\mathbf{v}_{ij}/dt \rangle_i = 1/3 \langle \mathbf{v}_{ij} \cdot \mathbf{f}_{ij} \rangle_i$. Hence, this thermostat changes the local temperature by two physical effects: by heat flow and by mechanical work. A similar mechanical work term in the temperature update was put forward by Phares and Srinivasa.¹⁶ In practical terms, by adding the second term in eq 10 with a negative value of μ , we gain the freedom to move the temperature up in Figure 3 and obtain the correct temperature for larger values of λ and, hence, for a shorter correlation time.

Does this mean that all problems with this thermostat are solved? A severe test is to study the ideal gas. For this system, the diffusion constant should diverge and the pair correlation should be 1. This is indeed the case with the Stoyanov–Groot thermostat, which is based on a global temperature. When a purely local temperature definition is used, however, this thermostat starts to compensate for the local temperature fluctuations that are natural within clusters of small numbers of particles. Just as with the Lowe–Anderson thermostat, this induces an interaction between the particles, which destroys their individual conservation of momentum. Consequently, the mean free path becomes finite and the diffusion constant no longer diverges. An example of this is shown in Figure 5, which gives the mean square displacement for an ideal gas at densities $\rho = 1, 3$, and 10 in a box of size $10 \times 10 \times 10$, with thermostat parameters $\alpha = 0.1$, $\lambda = 0.1$, and $\mu = 0$, over 50 000 time steps of size $\delta t = 0.05$. By fitting this to the solution of the Langevin equation,¹⁵ $\langle [r(t) - r(0)]^2 \rangle / 6t = D[1 + D(e^{-t/D} - 1)/t]$, where we have put $m = kT = 1$, the diffusion constant is obtained. This gives diffusion constants $D \approx 327$, $D \approx 381$, and $D \approx 400$ for the three densities, respectively, that is, large but finite values.

As a further check, the pair correlation function was studied. This shows a slight deviation from $g(r) = 1$, as shown in Figure 6. The deviation is quite small, but this deviation indicates that the thermostat induces an artificial conservative force between the particles, just as DPD does.

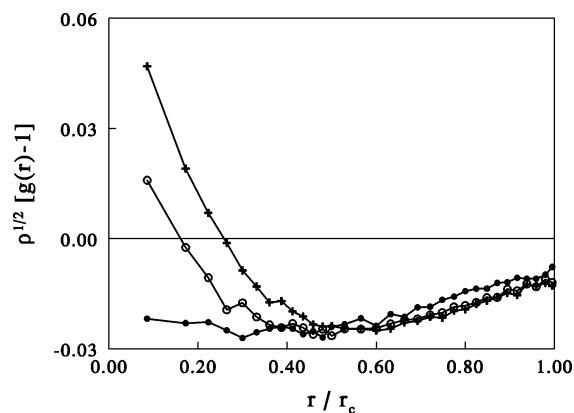


Figure 6. Total correlation function of the ideal gas at density $\rho = 1$ (+), $\rho = 3$ (O), and $\rho = 10$ (●).

For density $\rho = 10$, the maximum deviation is less than 0.009, but if for the same thermostat parameters the density is lowered, the deviations increase. This can be expected, because the mean number of neighbors of any particle is proportional to ρr_c^3 . Because the relative noise in the measured temperature of each particle is inversely proportional to the square root of the number of neighbors N , and because the deviations in the pair correlation are driven by these fluctuations, one may expect that the ideal-gas total correlation function scales as

$$g(r) - 1 \propto N^{-1/2} \propto r_c^{-3/2} \quad (11)$$

Hence, for a fixed cutoff radius and variable density, we expect that $\rho^{1/2}[g(r) - 1]$ is independent of the density. A glance at Figure 6 illustrates that, for a density range varying over a factor of 10, this scaling roughly holds for large r values ($r > r_c/2$). This implies that the errors introduced by the thermostat can be made arbitrarily small by increasing the cutoff range r_c . In practical terms, a cutoff that contains some 40 neighbors leads to systematic errors of about 0.5%.

5. Discussion and Conclusions

The thermostat introduced recently by Stoyanov and Groot¹⁵ is analyzed for inhomogeneous systems. In this thermostat, the temperature is obtained as an average over the whole system, and thus, it was anticipated that this could lead to a subtle nonlocal interaction.¹⁵ This will not destroy hydrodynamic behavior, because momentum is locally conserved, but the consequence of such nonlocality should be investigated to ascertain the method. Here, it is found that, although the system as a whole is simulated in an NVT ensemble, the Stoyanov–Groot thermostat locally conserves energy rather than temperature. Consequently, local temperature variations can be long-lived, although they do average out by thermal diffusion. To obtain a faster local temperature equilibration, a truly local thermostat must be introduced. To conserve momentum and, hence, to simulate hydrodynamic interactions, the thermostat must be Galilean invariant.

Such a local Galilean invariant thermostat is introduced here. This scheme is very much comparable to Dissipative Particle Dynamics,^{5–7} but the main difference is that no random numbers are used. This implies that the simulation method is faster than DPD, and because of the close

similarity to DPD, it sheds light on the known artifacts in the results for the ideal gas. Generally, all thermostats produce some artifacts, and the choice of method is usually a tradeoff between the nature of the artifacts and the problem investigated.

In the present thermostat, a local temperature is defined on each particle. Thus, a locally isothermal ensemble can be constructed. The local temperature is obtained from the local mean-square velocity around each particle. To arrive at a smoothly varying local temperature, a convolution over the past square velocities is taken by mixing the actual measured value with the smoothed temperature by a few percent. This is very similar to the original Nosé–Hoover algorithm. For a fast and accurate thermostat, the local smoothed temperature must be coupled to the actual temperature and its time derivative. This can be done with an update scheme based on the actual local temperature and that of the previous time step.

Simulations show that this local Nosé–Hoover algorithm has a similar artifact as Dissipative Particle Dynamics: the pair correlation function of the ideal gas is slightly distorted. This is attributed to the fact that the thermostat compensates fluctuations that are natural within a small cluster of particles. Consequently, when the cutoff range r_c for the square velocity average is increased, systematic errors decrease proportionally to $r_c^{-3/2}$. In practice, however, the error is on the order of a few tenths of a percent.

As mentioned above, the choice for a particular thermostat depends on a tradeoff of requirements. If it suffices to simulate in the local NVE ensemble with a global temperature control, the Stoyanov–Groot thermostat can be used. One special feature of this thermostat is that the fluid viscosity can be given any desired value, by switching between a low-viscosity local Nose–Hoover thermostat and a high-viscosity exchange process with probability P .¹⁵ For $P = 0$, the ideal gas has a divergent diffusion coefficient and zero viscosity, while for $P > 0$, it has a finite diffusion coefficient. Moreover, the temperature deviation from the required system temperature is at least an order of magnitude smaller than that for standard DPD, while the equilibrium properties of the system are very well reproduced. At the same time, it is computationally more efficient than self-consistent DPD,¹² by offering better temperature control and greater flexibility in terms of adjusting the diffusion coefficient and viscosity.

The same flexibility in simulated fluid viscosity is inherent in the present Galilean invariant thermostat, which simulates a truly locally isothermal system, but at the price of a slightly reduced accuracy in the temperature control. The presented thermostat can be applied in any conventional particle-based molecular dynamics simulation, including atomistic force fields. As a generalization, in a two-phase system, one can choose three different exchange frequencies P_{11} , P_{22} , and P_{12} . Thus, if phases 1 and 2 are mutually insoluble and if $P_{12} > P_{11} \geq P_{22}$, parameter P_{12} will introduce an excess surface viscosity of the resulting interface. With an extra surface-active component in the system, this would open up a new class of simulations where both bulk and surface viscosities and diffusion coefficients could be adjusted at will. Finally, simulation of dynamic intrusion and viscous fingering, as

well as spinodal decomposition in fluids of largely different viscosities, is straightforward.

References

- (1) Koga, T.; Kawasaki, K. *Physica A* **1993**, *196*, 389–415.
- (2) Qi, S.; Wang, Z. G. *Phys. Rev. E: Stat. Phys., Plasmas, Fluids, Relat. Interdiscip. Top.* **1997**, *55*, 1682–1697.
- (3) Shan, X. W.; Chen, H. D. *Phys. Rev. E: Stat. Phys., Plasmas, Fluids, Relat. Interdiscip. Top.* **1993**, *47*, 1815–1819.
- (4) Swift, M. R.; Orlandini, E.; Osborn, W. R.; Yeomans, J. M. *Phys. Rev. E: Stat. Phys., Plasmas, Fluids, Relat. Interdiscip. Top.* **1996**, *54*, 5041–5052.
- (5) Koelman, J. M. V. A.; Hoogerbrugge, P. J. *Europhys. Lett.* **1993**, *21*, 363–368.
- (6) Español, P.; Warren, P. *Europhys. Lett.* **1995**, *30*, 191–196.
- (7) Groot, R. D.; Warren, P. B. *J. Chem. Phys.* **1997**, *107*, 4423–4435.
- (8) Serrano, M.; Español, P. *Phys Rev E: Stat. Phys., Plasmas, Fluids, Relat. Interdiscip. Top.* **2001**, *64*, 046115.
- (9) Malevanets, A.; Kapral, R. *J. Chem. Phys.* **1999**, *110*, 8605–8613.
- (10) Nosé, S. *J. Chem. Phys.* **1984**, *81*, 511–519.
- (11) Hoover, W. G. *Phys. Rev. A: At., Mol., Opt. Phys.* **1985**, *31*, 1695–1697.
- (12) Pagonabarraga, I.; Hagen, M. H. J.; Frenkel, D. *Europhys. Lett.* **1998**, *42*, 337–382.
- (13) Andersen, H. C. *J. Chem. Phys.* **1980**, *72*, 2384–2393.
- (14) Lowe, C. P. *Europhys. Lett.* **1999**, *47*, 145–151.
- (15) Stoyanov, S. D.; Groot, R. D. *J. Chem. Phys.* **2005**, *122*, 114112.
- (16) Phares, D. J.; Srinivasa, A. R. *J. Phys. Chem. A* **2004**, *108*, 6100–6108.

CT050269E